Journal of Power Sources 196 (2011) 956–961

Contents lists available at ScienceDirect

Journal of Power Sources

journal homepage: www.elsevier.com/locate/jpowsour

Hydrazine electrooxidation on a composite catalyst consisting of nickel and palladium

Li Qiang Ye[a], Zhou Peng Li[a,*], Hai Ying Qin[a], Jing Ke Zhu[a], Bin Hong Liu[b]

[a] Department of Chemical and Biological Engineering, Zhejiang University, Hangzhou 310027, PR China
[b] Department of Materials Science and Engineering, Zhejiang University, Hangzhou 310027, PR China

ARTICLE INFO

Article history:
Received 17 July 2010
Received in revised form 27 August 2010
Accepted 27 August 2010
Available online 24 September 2010

Keywords:
Electrooxidation
Hydrazine
Composite catalyst
Synergy
Catalysis

ABSTRACT

A carbon nanotubes (CNTs) supported composite catalyst consisting of Pd and Ni (Pd–Ni/CNT) is synthesized by a chemical method. The electrocatalytic activities of Pd/CNT, Ni/CNT and Pd–Ni/CNT toward the hydrazine oxidation reaction (HOR) are evaluated by linear sweep voltammetry, electrochemical impedance spectroscopy and polarization measurement. The composite catalyst demonstrates higher electrocatalytic activity than its single-constituent catalysts due to the synergy between Ni and Pd. The Pd addition in the composite catalyst prevents oxidation of Ni so that the Pd–Ni/CNT electrode exhibits smaller reaction resistance to the HOR than the Ni/CNT and Pd/CNT electrodes.

1. Introduction

Recently, liquid fuels such as methanol, alkaline borohydride and hydrazine solutions have been used in the direct liquid fuel cells [1–3]. However, the direct methanol fuel cells (DMFCs) suffer from low power density and anode poisoning due to the methanol crossover during cell operation, and the CO absorption on anode catalysts [1]. Besides, the greenhouse gas (CO_2) generated from the methanol electrooxidation reaction is harmful to the environment. The direct borohydride fuel cells (DBFCs) have no problems related to catalyst poisoning, and the fuel crossover does not significantly influence the cell performance. However, the hydrogen evolution during operation is a serious problem because it not only decreases the fuel utilization and the cell performance but also makes the fuel cell system complicated [4,5]. Moreover, the borate generated from the borohydride electrooxidation makes refueling of DBFCs inconvenient [2].

Compared with methanol or borohydride as the fuel, hydrazine (N_2H_4) exhibits many advantages. Environment-benign nitrogen and water are the products from the direct hydrazine fuel cells (DHFCs):

$$N_2H_4 + O_2 \rightarrow N_2 + 2H_2O \quad E^0 = 1.61\,V \tag{1}$$

Nitrogen gas is easy to be expelled from the DHFCs. There is no catalyst poisoning in the DHFCs [3,6]. Moreover, the DHFCs demonstrate a high electric motive force of 1.61 V (close to 1.64 V of the DBFCs, higher than 1.21 V of the DMFCs). Some catalysts for the HOR have been developed [3,6–13]. It is reported that Pd is an effective catalyst [9,13]. Ni has high electrocatalytic activity at high temperature [10,11]. In our previous work [12], a composite catalyst containing Ni powder, Pd/C and hydrogen storage alloy has been used as the catalyst for the HOR at room temperature. However, the function of each constituent in the composite catalyst is not clear.

In order to understand the functions of the constituents in a composite catalyst toward the HOR, a catalyst consisting of Pd and Ni supported on carbon nanotubes (Pd–Ni/CNT) is synthesized. Based on materials characterization and electrochemical analyses via comparison of the composite catalyst with its single-constituent catalysts, a hypothesis of the synergy between Ni and Pd toward the HOR is suggested.

2. Experimental details

2.1. Catalyst preparation and characterization

The applied catalysts were prepared by depositing metallic particles on CNTs (from Beijing Cnano Technology, Ltd.) at 70 °C via the chemical reduction of Pd^{2+} and Ni^{2+} with hydrazine in an aqueous ethylene glycol (EG) solution, as suggested by Wu and Chen [14]. The metal contents in the obtained Pd/CNT, Ni/CNT

* Corresponding author. Tel.: +86 571 87951977; fax: +86 571 87953149.
E-mail address: zhoupengli@zju.edu.cn (Z.P. Li).

0378-7753/$ – see front matter © 2010 Elsevier B.V. All rights reserved.
doi:10.1016/j.jpowsour.2010.08.089

and Pd–Ni/CNT catalysts were measured to be 20 wt.%. The mass ratio of Pd to Ni in Pd–Ni/CNT was 1:1. The structure of these synthesized catalysts was characterized by powder X-ray diffraction (XRD) with a Rigaku-D/MAX-2550PC diffractometer using Cu Kα radiation (λ = 1.5406 Å). Their morphologies were observed with a JEM-2010 transmission electron microscope (TEM) operated at 200 kV.

2.2. Electrochemical analyses

Linear sweep voltammetry (LSV) and electrochemical impedance spectroscopy (EIS) tests were performed in a three-electrode system with the CHI 1140A electrochemical workstation (from CH Instruments, Inc.) and KFM2005 electrochemical workstation (from Kikusui electronics Corp.). The anode was prepared by pasting an anode ink onto a piece of Ni foam with a catalyst loading of 1 mg cm^{-2}. The anode ink was prepared by mixing the catalyst powders with water, ethanol and Nafion solution (5 wt.%) by a mass ratio of 1:3:3:7. A Pt wire and a saturated calomel electrode (SCE) were used as the counter electrode and reference electrode, respectively. Linear sweep voltammograms were recorded at a scan rate of 10 mV s^{-1}. EIS spectra were recorded under an applied current density of 2.75 mA cm^{-2} at 25 °C. The AC frequency was varied from 1 mHz to 1 kHz with an amplitude of 5 mV. All potentials were referred to SCE.

The anode polarization behavior was studied in a single cell with an active area of 6 cm^2 by the PFX2011S electrochemical workstation (Kikusui electronics Corp.). The anode was prepared by the same method as described in LSV and EIS measurements. The cathode was prepared by painting a cathode ink onto a piece of hydrophobic carbon cloth with a Pt loading of 0.25 mg cm^{-2}. The cathode ink was prepared by mixing the carbon support Pt powder (5 wt.% on Vulcan XC-72, E-Tek Co.) with water, ethanol and polytetrafluoroethylene (PTFE) solution (6 wt.%) by a mass ratio of 1:3:3:7. A Nafion membrane (N117) was used as the electrolyte to separate the anode and cathode in the cell. The membrane was pretreated by immersing in a boiling H_2O_2 solution (3 wt.%) for 1 h and then in a boiling de-ionized water for another 1 h. An alkaline hydrazine solution containing 2 M of N_2H_4 and 1 M of NaOH was used as the fuel. The electrode polarization was measured at a fuel flow rate of 50 ml min^{-1} and an oxygen flow rate of 150 ml min^{-1}.

3. Results and discussion

3.1. Catalyst characterization

Fig. 1 gives the XRD patterns of the synthesized catalysts. The diffraction patterns of Ni/CNT and Pd/CNT match the JCPDS files of PDF-04-0850 and PDF-87-0641, identifying the existence of the metallic Ni and Pd, respectively. The XRD pattern of Pd–Ni/CNT indicates the coexistence of the metallic Ni and Pd. Through Scherrer's equation from the full width half maximum (FWHM) of the diffraction peaks, the average size of Ni particles in Ni/CNT is estimated to be 16 nm, and the average sizes of Pd particles in Pd/CNT and Pd–Ni/CNT are estimated to be 8.8 and 10 nm, respectively.

TEM images of the synthesized catalysts are illustrated in Fig. 2. It can be seen that the metallic Pd is homogeneously distributed on CNTs in Pd/CNT, but metallic Ni exists in an aggregated form in Ni/CNT and Pd–Ni/CNT, probably caused by the magnetism of the metallic Ni. The sizes of metallic particles are close to the estimations according to the FWHM from XRD. The high resolution transmission electron microscopy (HRTEM) image of Pd–Ni/CNT reconfirms the coexistence of metallic Pd and Ni particles. Ni and Pd particles contact each other.

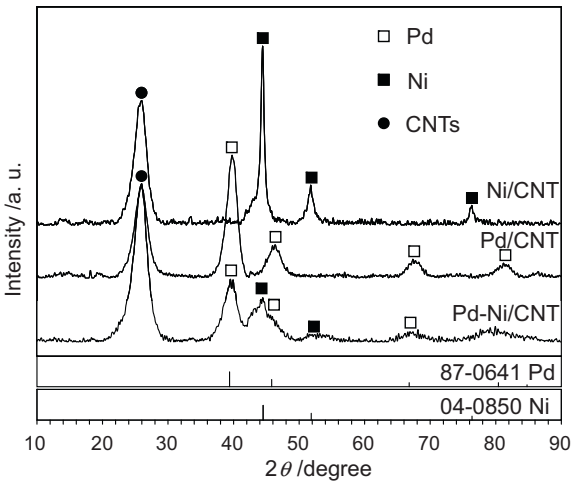

Fig. 1. XRD patterns of Ni/CNT, Pd/CNT and Pd–Ni/CNT.

3.2. Electrochemical evaluations

The transfer electron number of the HOR is determined by the N_2 evolution rate at a certain applied current during hydrazine electrooxidation as suggested in our previous work [15]. As shown in Fig. 3, the nitrogen evolution rates during the HOR on each catalyst are well fitted with the 4-electron-reaction of hydrazine electrooxidation:

$$N_2H_4 + 4OH^- \rightarrow N_2 + 4H_2O + 4e^- \quad E^0 = -1.21 \text{ V vs. SHE} \qquad (2)$$

Fig. 4 shows the polarization behavior of hydrazine electrooxidation at the Ni/CNT, Pd/CNT and Pd–Ni/CNT electrodes under 25 and 60 °C. The Pd–Ni/CNT electrode exhibits the smallest polarization. The EIS results as shown in Fig. 5 reveal that the reaction resistance of the hydrazine electrooxidation (evaluated by the diameter of semicircle at low frequencies in Nyquist plot) at the Pd–Ni/CNT electrode is smaller than that at the Ni/CNT and Pd/CNT electrodes. These results reveal that the composite catalyst has higher electrocatalytic activity than those single-constituent catalysts (Pd/CNT and Ni/CNT), though each constituent in Pd–Ni/CNT (0.5 mg cm^{-2} of Pd and Ni) is less than that in Pd/CNT and Ni/CNT (1 mg cm^{-2} of Pd or Ni). Based on these results, it is considered that the HOR at the Pd–Ni/CNT electrode proceeds via a different pathway from that at the Pd/CNT and Ni/CNT electrodes.

Figs. 6 and 7 show the hydrazine electrooxidation behavior at the Pd/CNT and Ni/CNT electrodes in alkaline solutions containing different contents of hydrazine, respectively. The anodic peak current (at −0.65 V in Fig. 6) increases with increasing the N_2H_4 concentration in the alkaline hydrazine solutions, referring to the HOR occurring at the Pd/CNT electrode. The anodic peak current (at 0.2 V in Fig. 7) increases with increasing the N_2H_4 concentration, referring to the HOR occurring at the Ni/CNT electrode. However, compared the Ni/CNT electrode with the $Ni(OH)_2$/CNT electrode, there is no distinct difference in the hydrazine electrooxidation behavior. This result implies that the surfaces of Ni particles in Ni/CNT have been covered by $Ni(OH)_2$. It is considered that the poor electrocatalytic activity of Ni/CNT is caused by the surface oxidation of the Ni particles during the HOR at ambient condition.

It is known that Ni has a high electrocatalytic activity toward the HOR at high temperatures [10,11]. Ni(II) can be chemically reduced to metallic Ni in an alkaline hydrazine solution at high temperature, as described in the catalyst preparation and characterization. It is considered that the metallic Ni surface can be reserved when the DHFCs operate at higher temperatures. In order to prove this deduction, the linear potential sweeps of the Ni/CNT

electrode were performed after the electrode was immersed in the alkaline hydrazine solution (containing 2 M N_2H_4 and 1 M NaOH) for 20 min under 60 °C. As shown in Fig. 8, the anodic current peaks appear at lower potentials where hydrazine could not be oxidized on Ni at 25 °C. The insert figure in Fig. 8 gives the cyclic voltammogram of the Ni/CNT electrode in the 1 M NaOH solution, which reveals that Ni could be electrooxidized at lower potentials. Therefore, A sequent process of electrochemical reaction occurs at

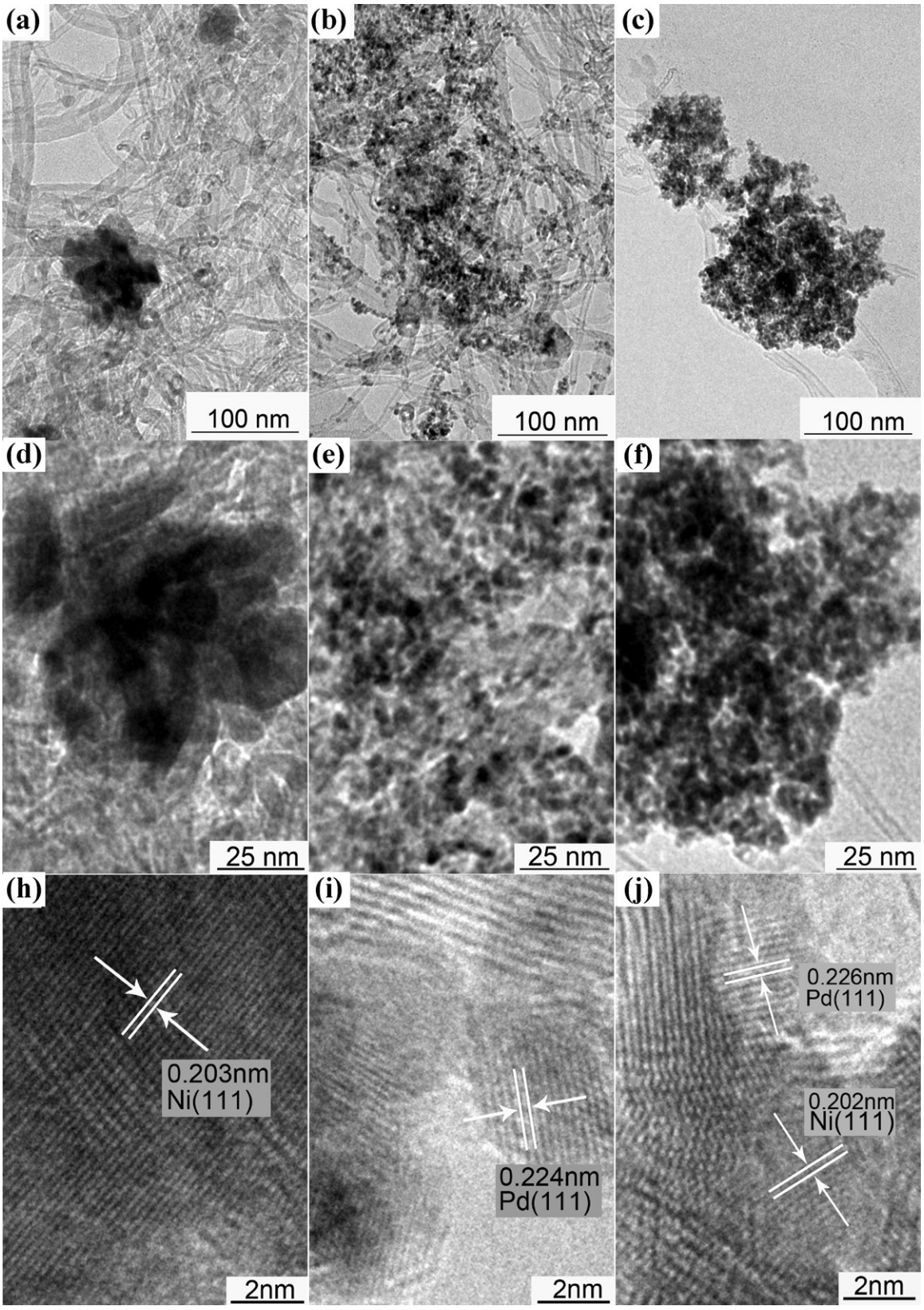

Fig. 2. TEM (a–f) and HRTEM (h–j) images of Ni/CNT (a, d, and h), Pd/CNT (b, e, and i) and Pd–Ni/CNT (c, f, and j).

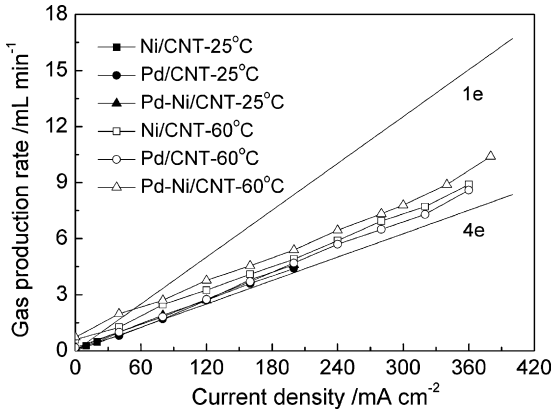

Fig. 3. Gas evolution rates during the HOR on Ni/CNT, Pd/CNT and Pd–Ni/CNT at 25 and 60 °C.

the Ni/CNT electrode in the hydrazine solution (5 mM N_2H_4): the HOR on metallic Ni, the Ni electrooxidation reaction, and then the HOR on $Ni(OH)_2$ according to the linear sweep voltammograms. As shown in Fig. 8, the anodic current at lower potential increases significantly with increasing the concentration of N_2H_4 in the alkaline hydrazine solutions, indicating that hydrazine has been electrooxidized on metallic Ni under high temperature. The anodic current peak around −0.825 V can be attributed to the HOR on metallic Ni.

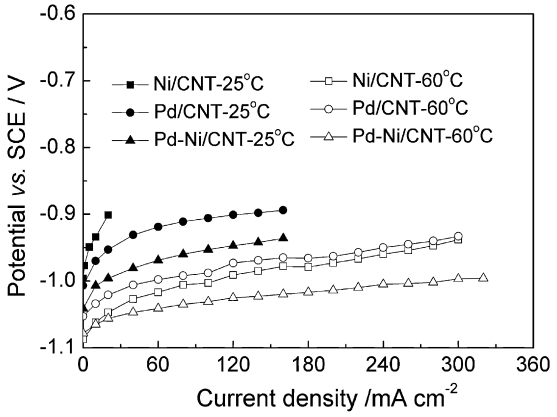

Fig. 4. Polarization behavior of hydrazine electrooxidation in the alkaline solution (2 M N_2H_4–1 M NaOH) on Ni/CNT, Pd/CNT and Pd–Ni/CNT.

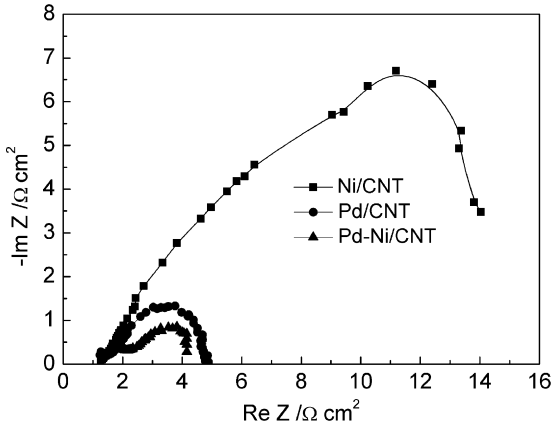

Fig. 5. Electrochemical impedance spectra of the HOR at the Ni/CNT, Pd/CNT and Pd–Ni/CNT electrodes in an alkaline solution containing 2 M of N_2H_4 and 1 M of NaOH at 25 °C.

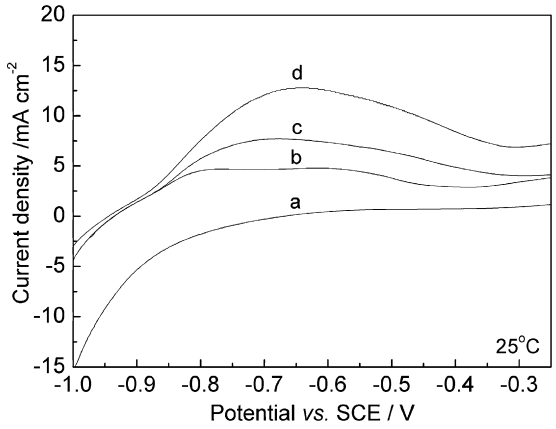

Fig. 6. LSVs of hydrazine at the Pd/CNT electrode in alkaline solutions (1 M NaOH) containing no N_2H_4 (a); 5 mM N_2H_4 (b); 10 mM N_2H_4 (c); 20 mM N_2H_4 (d).

Fig. 9 shows the linear sweep voltammograms of hydrazine at the Pd/CNT and Ni/CNT electrodes with different catalyst contents. The decrease of Pd content in the Pd/CNT electrode leads to a decrease of the anodic current, whereas the Ni content in the Ni/CNT electrode shows little effect on the anodic current. However, the Pd–Ni/CNT electrode demonstrates higher electrocatalytic activity than the Ni/CNT and Pd/CNT electrodes, though the Pd

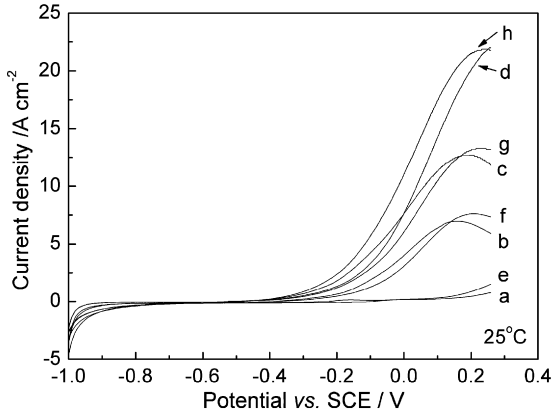

Fig. 7. LSVs of hydrazine at the Ni/CNT (a–d) and $Ni(OH)_2$/CNT (e–h) electrodes in alkaline solutions (1 M NaOH) containing no N_2H_4 (a and e); 5 mM N_2H_4 (b and f); 10 mM N_2H_4 (c and g); 20 mM N_2H_4 (d and h).

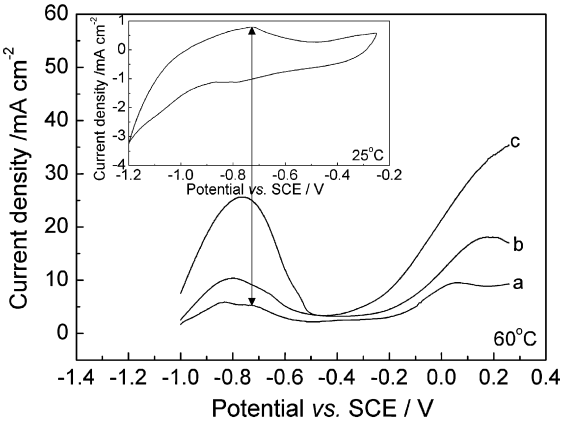

Fig. 8. LSVs of hydrazine at the Ni/CNT electrode in alkaline hydrazine solutions (1 M NaOH) containing 5 mM N_2H_4 (a); 10 mM N_2H_4 (b); 30 mM N_2H_4 (c). The electrode has been immersed in the solution (containing 2 M N_2H_4 and 1 M NaOH) for 20 min under 60 °C before testing. The insert figure shows the cyclic voltammogram of the Ni/CNT electrode in the 1 M NaOH solution.

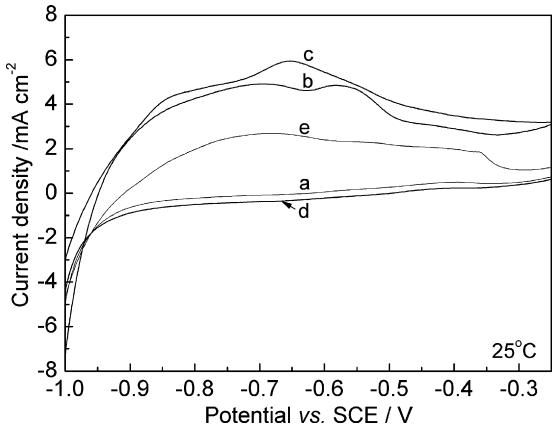

Fig. 9. LSVs of hydrazine at (a) the Ni/CNT electrode (1 mg cm^{-2} of Ni), (b) the Pd/CNT electrode (1 mg cm^{-2} of Pd), (c) the Pd–Ni/CNT electrode (0.5 mg cm^{-2} of Pd, 0.5 mg cm^{-2} of Ni), (d) the Ni/CNT electrode (0.5 mg cm^{-2} of Ni), (e) the Pd/CNT electrode (0.5 mg cm^{-2} of Pd) in the alkaline hydrazine solution (5 mM N_2H_4–1 M NaOH).

content in Pd–Ni/CNT is half of that in Pd/CNT. Obviously, a simple combining effect of the Pd/CNT electrode (0.5 mg cm^{-2} of Pd) and the Ni/CNT electrode (0.5 mg cm^{-2} of Ni) can not explain the hydrazine electrooxidation behavior at the Pd–Ni/CNT electrode containing the same amount of Pd and Ni as shown in Fig. 9. It is considered that the HOR on Pd–Ni/CNT proceeds with a synergy of Ni and Pd toward the HOR.

3.3. Synergy between Pd and Ni

The Pd–Ni/CNT electrode at 25 °C demonstrates an anodic behavior similar to the Ni/CNT electrode at 60 °C as shown in Fig. 10(a). There are two anodic current peaks. The anodic current peak around −0.825 V can be attributed to the hydrazine electrooxidation as described above, and the peak at −0.72 V can be attributed to the Ni electrooxidation because a redox couple appears in the alkaline solution without N_2H_4 addition as shown in Fig. 10(b). The unbalanced relationship between the cathodic and anodic currents is caused by the hydrogen evolution in the cathodic process because hydrogen generates at more negative potential than the Ni(II) elec-

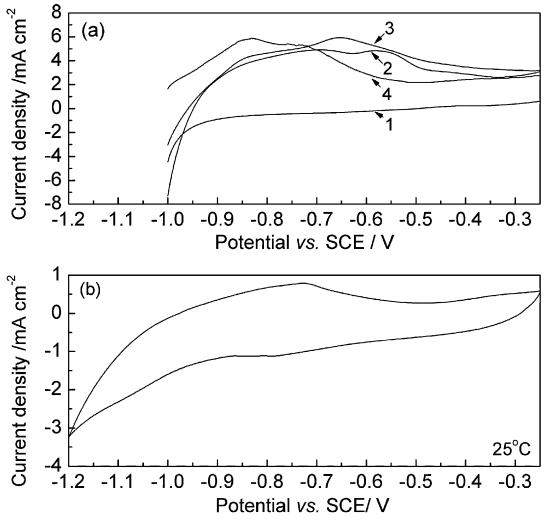

Fig. 10. (a) LSVs of hydrazine in the alkaline solution (5 mM N_2H_4–1 M NaOH) at 25 °C using (1) Ni/CNT, (2) Pd/CNT, (3) Pd–Ni/CNT electrodes, and at 60 °C using (4) Ni/CNT electrode after being immersed in the solution (2 M N_2H_4–1 M NaOH) for 20 min under 60 °C. (b) Cyclic voltammogram of the Ni/CNT electrode in the 1 M NaOH solution at 25 °C.

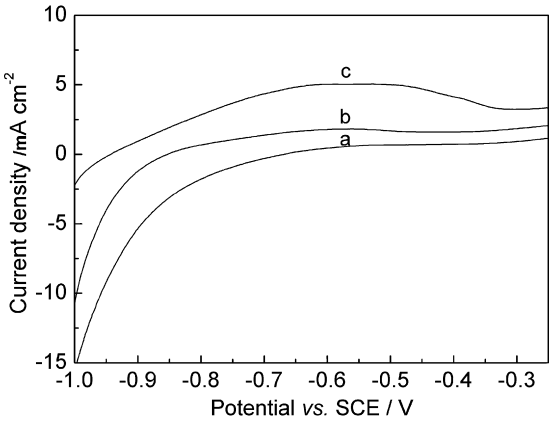

Fig. 11. LSVs of the Pd/CNT electrode in 1 M NaOH after being immersed in 2 M N_2H_4–1 M NaOH solution with different intervals, a: 0 min; b: 10 min; c: 20 min.

troreduction regarding to theoretical potential calculation. These results are coincident with the results that Ni electrooxidation easily occurs in alkaline media by following reaction [16,17]:

$$Ni + 2OH^- \rightarrow Ni(OH)_2 + 2e^- \quad (3)$$

and the Ni electrode has practically no ability to take out hydrogen from hydrazine molecules at room temperature [18].

Jung et al. [19] suggested a palladium-doped double-walled silica nanotubes (SNTs) as a hydrogen storage material. It was reported that the Pd metal could adsorb hydrogen as mobile atoms [20], and the Pd hydride could be formed at 0.08 V vs. RHE (corresponding to −0.8 V vs. SCE) in a 0.1 M NaOH solution [21]. Skowroński et al. [22] found that hydrogen adsorbed in Pd catalyst was electrooxidized at −0.4 V vs. Hg/HgO in 6 M NaOH (corresponding to −0.55 V vs. SCE). These results imply that Pd hydride could be formed when a Pd electrode was immersed into a hydrazine solution.

In order to identify the Pd hydride formation, the linear potential sweep of the Pd/CNT electrode was performed in the NaOH solution (1 M) after the electrode was immersed in the alkaline hydrazine solution (2 M N_2H_4, 1 M NaOH) with different intervals. The electrode was washed with a NaOH solution (1 M) for several times to make sure that no N_2H_4 left on the electrode before testing. It was found that the oxidation peak current around −0.55 V increased with increasing the immersing interval as shown in Fig. 11, which indicated that Pd hydride had been formed during immersing the Pd/CNT electrode in the alkaline hydrazine solution, according to the Pd hydride electrooxidation reaction [22].

From these results and discussion as mentioned above, it can be concluded that the HOR on Pd–Ni/CNT takes place as follows:

(1) Pd absorbs hydrogen from hydrazine to form Pd hydride;
(2) Pd hydride reacts with $Ni(OH)_2$ on the surfaces of Ni particles to form metallic Ni through a microcell reaction between Pd hydride particles and Ni hydroxide on Ni particles:

$$2PdH_x + xNi(OH)_2 \rightarrow xNi + 2Pd + 2xH_2O \quad (4)$$

(3) hydrazine electrooxidation reaction occurs on Ni and Pd.

According to the theoretical calculation from Gibbs free energy [23] ($\Delta G^\circ = -17$ KJ mol^{-1} < 0 when $x = 0.5$), reaction (4) is feasible. It is believed that the Pd existence in the composite catalyst prevents Ni oxidation in alkaline hydrazine solutions during the HOR due to the formation of Pd hydride and the feasible reaction (4). Because metallic Ni has higher electrocatalytic activity toward the HOR than Pd [3,10], the Pd–Ni/CNT electrode demonstrates smaller

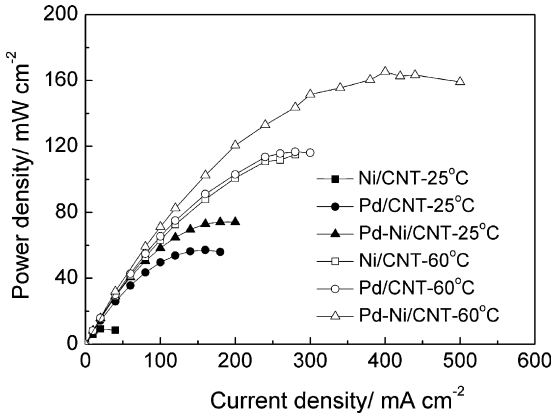

Fig. 12. Cell performances of the DHFCs using Ni/CNT, Pd/CNT and Pd–Ni/CNT as the anode catalysts and Pt/C as the cathode catalyst at 25 and 60 °C.

reaction resistance of hydrazine electrooxidation than the Ni/CNT and Pd/CNT electrodes at room temperature.

Fig. 12 exhibits the cell performances of the DHFCs using Ni/CNT, Pd/CNT and Pd–Ni/CNT as the anode catalysts and Pt/C as the cathode catalyst. The cell performance increases with increasing the operation temperature because high operation temperature is beneficial to both the HOR and the oxygen reduction reaction (ORR). It is noted that the performance improvement of the DHFC using Pd–Ni/CNT at 60 °C is more significant than that at 25 °C. It is because that Ni could exist in metallic state during the HOR according to the reaction (4) and the following reaction:

$$N_2H_4 + 2Ni(OH)_2 \rightarrow 2Ni + N_2 + 4H_2O \quad (5)$$

Therefore, Pd and Ni exhibit more significant synergy to improve the electrocatalytic activity of Pd–Ni/CNT toward the HOR at higher operation temperatures. As a result, the DHFC using Pd–Ni/CNT shows higher performance improvement at higher temperatures than at low temperature.

4. Conclusions

CNTs supported Ni, Pd and Pd–Ni catalysts are successfully prepared by reduction of Pd and Ni precursors with hydrazine in an aqueous ethylene glycol solution. Pd–Ni/CNT demonstrates higher electrocatalytic activity toward the HOR than Ni/CNT and Pd/CNT due to the synergy between Ni and Pd. The HOR on Pd–Ni/CNT takes place through following steps:

(1) Pd absorbs hydrogen from hydrazine to form Pd hydride;
(2) Pd hydride reacts with $Ni(OH)_2$ existing on surfaces of Ni particles to form metallic Ni surfaces;
(3) hydrazine electrooxidation reaction occurs on metallic Ni and Pd.

The performance measurements prove that the synergy between Ni and Pd plays an important role in the performance improvement of the DHFCs.

Acknowledgments

This work is financially supported by Hi-tech Research and Development Program of China (863), grant no. 2007AA05Z144; Doctoral fund from Education Ministry of China (20070335003); and the National Natural Science Foundation of China, grant nos. 20976156 and 50971114.

References

[1] X.M. Ren, M.S. Wilson, S. Gottesfeld, J. Electrochem. Soc. 143 (1996) L12–L15.
[2] B.H. Liu, Z.P. Li, J. Power Sources 187 (2009) 291–297.
[3] K. Yamada, K. Yasuda, H. Tanaka, Y. Miyazaki, T. Kobayashi, J. Power Sources 122 (2003) 132–137.
[4] B.H. Liu, Z.P. Li, J.K. Zhu, S. Suda, J. Power Sources 183 (2008) 151–156.
[5] U.B. Demirci, J. Power Sources 169 (2007) 239–246.
[6] K. Yamada, K. Asazawa, K. Yasuda, T. Ioroi, H. Tanaka, Y. Miyazaki, T. Kobayashi, J. Power Sources 115 (2003) 236–242.
[7] A. Abbaspour, M.A. Kamyabi, J. Electroanal. Chem. 576 (2005) 73–83.
[8] K. Asazawa, K. Yamada, H. Tanaka, A. Oka, M. Taniguchi, T. Kobayashi, Angew. Chem. Int. Ed. 42 (2007) 8170–8173.
[9] N. Maleki, A. Safavi, E. Farjami, F. Tajabadi, Anal. Chim. Acta 611 (2008) 151–155.
[10] K. Asazawa, T. Sakamoto, S. Yamagachi, K. Yamada, H. Fujikawa, H. Tanaka, K. Oguro, J. Electrochem. Soc. 156 (2009) B509–B512.
[11] S.J. Lao, H.Y. Qin, L.Q. Ye, B.H. Liu, Z.P. Li, J. Power Sources 195 (2010) 4135–4138.
[12] H.Y. Qin, Z.X. Liu, Y.F. Guo, Z.P. Li, Int. J. Hydrogen Energy 35 (2010) 2868–2871.
[13] A. Serov, C. Kwak, Appl. Catal. B: Environ. 98 (2010) 1–9.
[14] S.H. Wu, D.H. Chen, J. Colloid Interface Sci. 259 (2003) 282–286.
[15] W.X. Yin, Z.P. Li, J.K. Zhu, H.Y. Qin, J. Power Sources 182 (2008) 520–523.
[16] A. Seghiouer, J. Chevalet, A. Barhoun, F. Lantelme, J. Electroanal. Chem. 442 (1998) 113–123.
[17] M. Fleischmann, K. Korinek, D. Pletcher, J. Electroanal. Chem. 34 (1972) 499–503.
[18] Y. Fukumoto, T. Matsunaga, T. Hayashi, Electrochim. Acta 26 (1981) 631–636.
[19] J.H. Jung, J.A. Rim, S.J. Lee, S.J. Cho, S.Y. Kim, J.K. Kang, Y.M. Kim, Y.J. Kim, J. Phys. Chem. C 111 (2007) 2679–2682.
[20] E.J. Nowak, J. Phys. Chem. 73 (1969) 3790–3794.
[21] S.I. Pyun, T.H. Yang, Electrochim. Acta 41 (1996) 843–848.
[22] J.M. Skowroński, A. Czerwiński, T. Rozmanowski, Z. Rogulskic, P. Krawczyk, Electrochim. Acta 52 (2007) 5677–5684.
[23] J.A. Dean, Lange's Handbook of Chemistry, 15th ed., McGraw-Hill, 1999.